IN VIVO CYCLIC LOADING AS A POTENT STIMULATORY SIGNAL FOR BONE FORMATION INSIDE TISSUE ENGINEERING SCAFFOLDS

Alireza Roshan-Ghias[1], Alexandre Terrier[1], Pierre-Etienne Bourban[2] and Dominique P. Pioletti[1*]

[1] Laboratory of Biomechanical Orthopedics, [2]Laboratory of Composite and Polymer Technology, EPFL, Lausanne, Switzerland

Abstract

In clinical situations, bone defects are often located at load bearing sites. Tissue engineering scaffolds are future bone substitutes and hence they will be subjected to mechanical stimulation. The goal of this study was to test if cyclic loading can be used as stimulatory signal for bone formation in a bone scaffold. Poly(L-lactic acid) (PLA)/ 5% β-tricalcium phosphate (β-TCP) scaffolds were implanted in both distal femoral epiphyses of eight rats. Right knees were stimulated (10N, 4Hz, 5 min) five times, every two days, starting from the third day after surgery while left knees served as control. Finite element study of the *in vivo* model showed that the strain applied to the scaffold is similar to physiological strains. Using micro-computed tomography (CT), all knees were scanned five times after the surgery and the related bone parameters of the newly formed bone were quantified. Statistical modeling was used to estimate the evolution of these parameters as a function of time and loading. The results showed that mechanical stimulation had two effects on bone volume (BV): an initial decrease in BV at week 2, and a long-term increase in the rate of bone formation by 28%. At week 13, the BV was then significantly higher in the loaded scaffolds.

Keywords: Bone tissue engineering, osteogenesis, animal model, mechanical stimulation.

* Address for correspondence:
Dominique Pioletti
EPFL/STI/IBI/LBO
Station 15
CH-1015 Lausanne,
Switzerland

E-mail: dominique.pioletti@epfl.ch

Introduction

The growing need for bone substitutes is the driving motivation for researchers to develop bone scaffolds and improve the process of bone regeneration. The latter has been the focus of many studies and some techniques have been proposed for enhancing osteogenesis inside bone scaffolds, like seeding scaffolds with mesenchymal stem cells (Meinel *et al.,* 2004) or with fetal bone cells (Pioletti *et al.,* 2006), delivering growth factors using scaffolds (Murakami *et al.,* 2002; Richardson *et al.,* 2001) or pre-mineralization in *in vitro* bioreactors (Cartmell *et al.,* 2003). All of these methods have been successful to some extent, but they have certain disadvantages. For instance, the high cost of the final product in all these techniques is certainly an important issue.

Mechanical stimulation is another potential method for enhancing bone regeneration that can be employed by designing the scaffold and controlling the external load accordingly. It has long been known that mechanical stimulation has regulatory effects on bone cells and architecture of bone (Forwood *et al.,* 1996; Turner *et al.,* 1994). *In vitro* studies suggest that fluid flow enhances expression of the osteoblastic phenotype (Cartmell *et al.,* 2003; Sikavitsas *et al.,* 2003; Tanaka *et al.,* 2005; Zhao *et al.,* 2007), proliferation of mesenchymal stromal cells (Song *et al.,* 2007) and mineralization (Bancroft *et al.,* 2002; Goldstein *et al.,* 2001; Sikavitsas *et al.,* 2005). However, an excessive amount of fluid flow or cyclic compression may decrease the number of cells or have no osteogenic effect (Cartmell *et al.,* 2003; Rath *et al.,* 2008; van Eijk *et al.,* 2008). Although *in vitro* studies help us understand the mechanisms of mechanotransduction, the cellular events in *in vivo* conditions are more complex and greatly unknown. In particular, drilling of bone initiates a bone healing cascade that results in different cellular activities and chemical environment compared to quiescent *in vitro* conditions.

A frequently used model to study the effect of mechanical stimulation on bone regeneration *in vivo* is the bone chamber. Using bone chambers, some researchers have reported that mechanical loading enhances bone formation (Guldberg *et al.,* 1997; Lamerigts *et al.,* 2000; van der Donk *et al.,* 2002), and some observed that loading inhibits bone formation (Tagil and Aspenberg, 1999). Duty and coworkers (Duty *et al*., 2007) used a subcutaneous bone chamber and found that cyclic loading of mesenchymal stem cell seeded scaffolds enhances the mineralization.

In the present study, we hypothesized that mechanical stimulation enhances bone regeneration in scaffold. Distal femoral epiphysis of rat was used as an *in vivo* model to study the effect of mechanical stimulation on bone formation in a polymeric scaffold. Micro computed
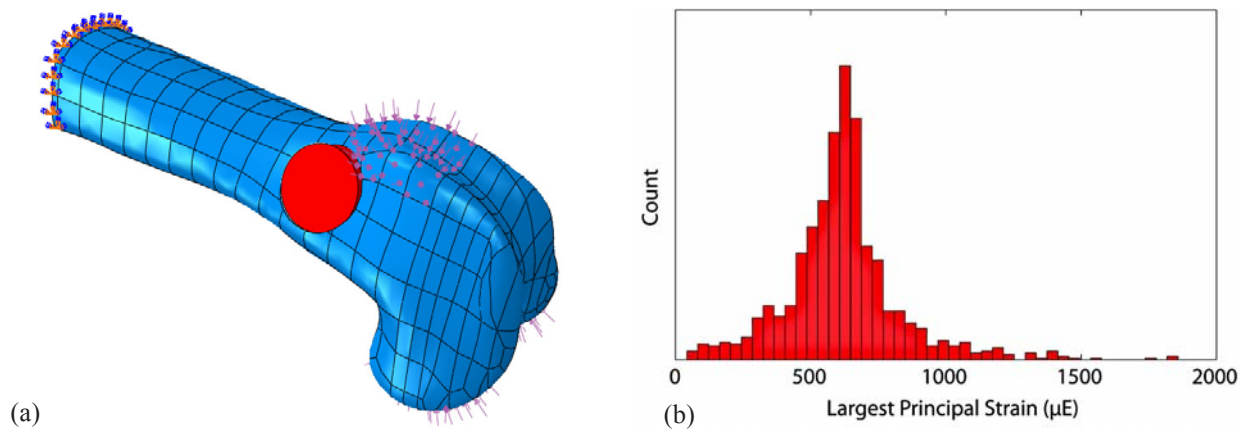
Fig. 1. (a) Distal femoral epiphysis model where bone is in blue and scaffold is in red. The loading is shown by violet arrows on anterior and posterior sides of the distal femur. (b) The histogram of largest principal strain in scaffold. Count represents the number of elements having the same value of strain.

tomography (CT) was used to study bone formation *in vivo*. Longitudinal analysis was then employed to model and investigate the effect of loading on bone formation.

Materials and Methods

Finite element modeling
Finite element modeling was performed to determine the magnitude of load to be applied in *in vivo* experiment. A rat femur was scanned using a SkyScan 1076 *in vivo* scanner (SkyScan, Kontich, Belgium), and reconstructed using NRecon and CTAN software (SkyScan) and prepared for meshing using Geomagic (Geomagic, Research Triangle Park, NC, USA). The obtained geometry was imported to ABAQUS (Simulia, Providence, RI, USA) for numerical analysis (Fig. 1a). The scaffold was positioned inside the lateral distal femoral epiphysis based on the feasibility studies done on several rat cadavers. The bone and the scaffold were considered to be linear elastic materials. Mechanical properties of cortical and trabecular bone were obtained from the literature (Hogan *et al.*, 2000). The mechanical properties of the scaffold were previously measured and reported by Blecha (Blecha, 2007) (E=20 MPa, υ=0.3). As the boundary condition, the proximal end of the bone was fixed. Based on the cadaver studies, it was assumed that no slip occurs at the interface between scaffold and bone. Loading orientation was based on the positioning of the leg in the loading device. Different magnitudes of load were applied to the anterior and posterior parts of distal femur and the average largest principal strain inside the scaffold was calculated. It was found that 10 N of loading results in strain of 622 ±220 µε inside the scaffold, which is close to physiological strains in human tibia while walking (Burr *et al.*, 1996). Fig. 1b shows the histogram of the distribution of strain inside the scaffold.

Scaffold fabrication
The processing of foams, as well as analyses of scaffold morphology, was carried out as described elsewhere (Mathieu *et al.*, 2006). In short, poly(L-lactic acid) (PLA)

pellets and β-tricalcium phosphate (β-TCP) ceramic powder (5% weight) were mixed, and further melt-extruded using a micro-compounder. Foaming was then carried out with supercritical CO_2, in a custom made high-pressure chamber. Once CO_2 was dissolved in PLA, foaming was achieved by sudden gas release, which induces bubble nucleation and their growth. Finally the controlled cooling till room temperature fixes the porous structure. The *in vitro* biocompatibility of the obtained scaffold has been verified (Montjovent *et al.*, 2005) as well as its *in vivo* performance in rat (Montjovent *et al.*, 2008; Montjovent *et al.*, 2007). Cylindrical scaffolds (3 mm in diameter and height) were cored from the foam and sterilized using ethylene oxide gas. Prior to surgery, scaffolds were perfused with phosphate-buffered saline (PBS) to remove the air bubbles trapped inside.

Surgical procedure
Both distal femoral epiphyses of eight female Wistar rats (weight 245-250 g) were operated (Veterinary Authority from the Canton of Vaud, authorization No. 2140) following a protocol already used in our laboratory (Montjovent *et al.*, 2008; Peter *et al.*, 2006). The animal was anesthetized using Isoflorane gas and both legs were shaved and sterilized. Five ml of Morphasol (Graeub Veterinary Products, Bern, Switzerland) were injected subcutaneously as analgesia. The lateral side of the knee joint was opened and after exposing the distal femur, the location of the hole was marked on the bone based on the distance from the joint and the insertion point of ligaments. The hole (3 mm in diameter and depth) was made using a hand drill and the scaffold was implanted inside the hole. Finally, the surrounding was washed with saline, the muscles were sutured, and the skin was closed using surgical clips (Stoelting, Wood Dale, IL, USA). No antibiotic was given after the surgery, but to reduce the pain, Dafalgan (Bristol-Myers Squibb, New York, NY, USA) was administered in water for 3 days post-surgery.

Mechanical stimulation
Fig. 2 shows the timeline of the experiment. Three days after the surgery, the loading of the knee started using a
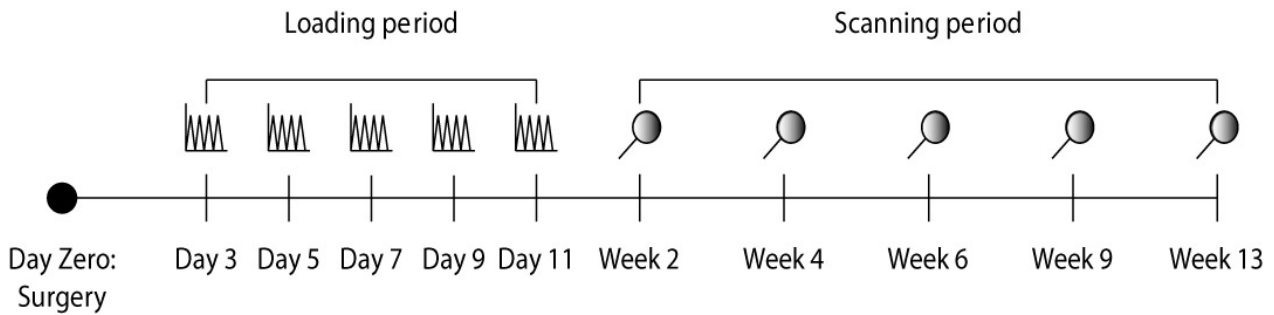
Fig. 2. The timeline of the *in vivo* experiment.

compression machine previously developed in our laboratory (Stadelmann *et al.*, 2007) (Fig. 3a). The right leg of each animal was loaded and the left leg was kept unloaded as control. The animals were anesthetized by Isoflorane gas for the loading period. The knee and the heel of the right leg were placed in the grip of the machine and the loading was applied as a triangle waveform with amplitude of 10 N at 4 Hz for 5 minutes. The loading was done five times, every two days.

Bone formation evaluation

The bone formation was quantified using a Skyscan 1076 *in vivo* micro-CT scanner (Skyscan) at 5 time points: 2, 4, 6, 9, and 13 weeks after the surgery. Animals were kept under anesthesia by Isoflorane during the scanning. Each leg was scanned separately along with two hydroxyapatite phantoms with densities of 0.25 and 0.75 g.cm^{-3}, 8 mm in diameter (Gloor Instruments, Uster, Switzerland) and a tube of water for later calibration of bone mineral density (BMD) (Fig. 3b). The legs were stretched and confined using tape to isolate the knee joint. All animals were scanned using the same parameters (18 μm, 80 kV, 124 μA, 1 mm Al filter, 600 ms exposure time, 14 min of scanning) at all time points. The local absorbed dose rate is reported to be 0.043 Gy/min for hindlimb knee of rat in identical scanning conditions to ours (data provided by SkyScan). Thus, a 14 min scan will result in radiation dose of 0.6 Gy. The reconstruction and analysis was done using NRecon and CTan software (Skyscan), respectively. A second order polynomial correction algorithm was used to reduce beam-hardening effect for all samples. Since the scaffold is undistinguishable inside the hole, the region of interest (ROI) was selected as the volume of the hole. The CT numbers were first converted to Hounsfield unit (HU) using scans of water tubes, and then to bone mineral density (BMD) using phantoms. Based on visual inspections of tomograms, a threshold value of 0.5 gr/cm^3 was chosen to segment bone in the scaffold. Accordingly, bone volume (BV), BMD, interception surface (IS), and trabecular thickness (Tb.Th) were measured for each ROI. Interception surface is the surface of the ROI intercepted by solid binarised objects, that is, the part of the volume of interest boundary surface that runs through solid objects.

Statistical analysis

Linear mixed-effect modeling was used to model the

evolution of BV, BMD, IS, and Tb.Th as a function of time and loading (Diggle *et al.*, 2002). The linear model can be written as

$$y_{ijk} = (\beta_0 + b_{0i}) + (\beta_1 + b_{1i}) F_j + (\beta_2 + b_{2i}) T_k + \beta_{12} F_j T_k + \varepsilon_{ijk} \quad (1)$$

where $i=1,2,3,...,8$ is the number of rats, $j=0,1$ is the index for control and loaded groups, respectively, and $k=1,2,3,..,5$ is the index for time points. β_0, β_1, β_{12}, β_2 are the fixed-effect variables, b_{0i}, b_{1i}, b_{2i} are the random-effect variables, and ε_{ijk} is the within-subject error term. β_0 is a constant, β_1 represents the time-independent effect of loading, β_2 the loading-independent effect of time, and β_{12} the time-dependent effect of loading. β_{0i}, β_{1i}, β_{2i} are the corresponding associated random effects. y_{ijk} is the response (BV, BMD, IS, or Tb.Th), F_j is a dummy variable which is 0 for control and 1 for loading group, and T_k is the time of measurement in days after the surgery. It is assumed that $b_i = (b_{0i}, b_{1i}, b_{2i})^T$ are independent and identically distributed with a $N(0, \sigma^2 I)$ distribution, where $\sigma^2 I$ represents the covariance matrix for random effects. Furthermore, we assume that the ε_{ijk} are independent and identically distributed with a $N(0, \sigma^2)$ distribution, independent of the b_i. Restricted maximum likelihood method was used for parameter estimation (Pinheiro and Bates, 2004).

Repeated measures analysis of covariances (ANCOVA) was used to evaluate the differences between the control and loaded groups. Differences between means at the 5% and 1% confidence level ($p<0.05$, and $p<0.01$) were considered statistically significant and highly significant, respectively. All statistical analyses were done in S-PLUS (Tibco, Palo Alto, CA, USA).

Results

No complication occurred during or after the surgeries and all animals could use their legs immediately after the surgery. Implanting scaffold was successful except in three legs. In one case, the scaffold was loose inside the left leg resulting in almost no bone formation inside. In another rat, the scaffolds did not completely fit inside both holes resulting in significantly lower bone formation. Therefore, these two animals were put aside from the experiment.
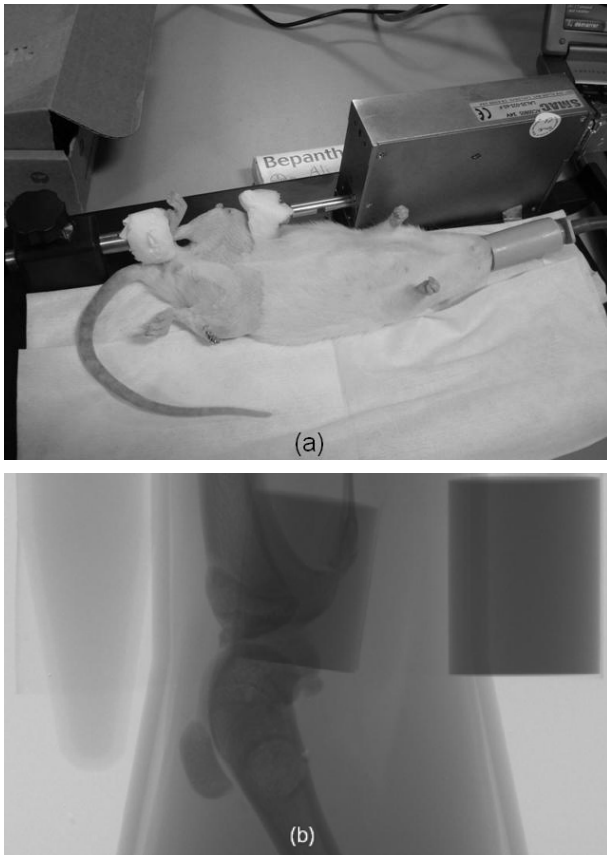
Fig. 3. (a) Anesthetized rat positioned in the loading machine, (b) x-ray of knee joint, two phantoms, and a tube of water.
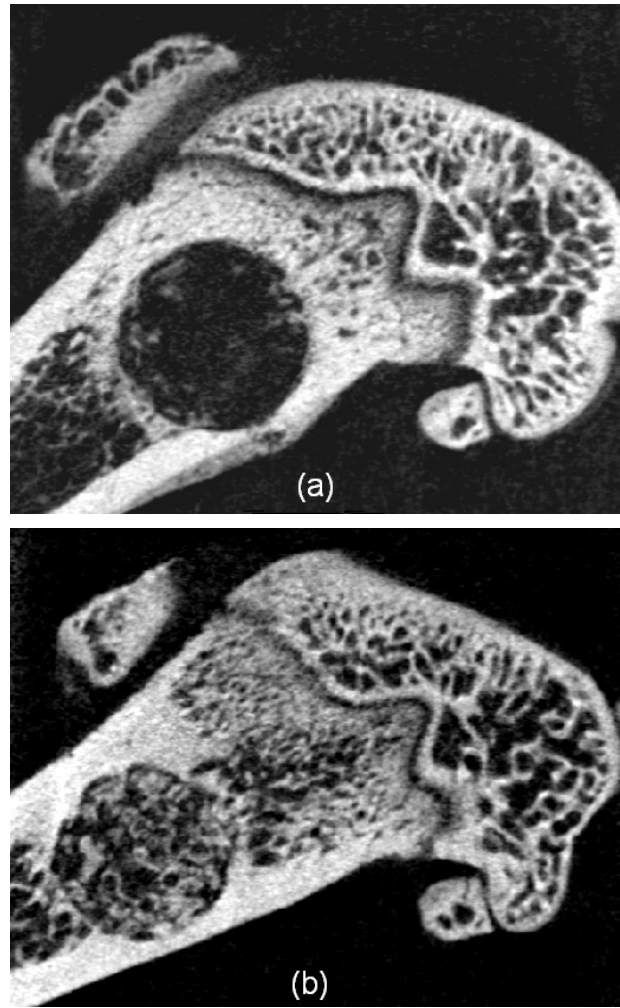

Fig. 4. CT slice of a loaded distal femoral at (a) 2 weeks, (b) 13 weeks. Note that both figures are from the same leg of the same animal and the change in the scaffold position is due to the growth of the animal during 11 weeks.

Table 1. Linear mixed-effect modeling of bone parameters

	β_0			β_1			β_2			β_{12}		
	Mean	SE	*p*-value	Mean	SE	*p*-value	Mean	SE	*p*-value	Mean	SE	*p*-value
BV	0.69	0.22	< 0.0001	-0.81	0.35	0.02	0.083	0.0056	< 0.0001	0.023	0.0052	0.0001
BMD	0.69	0.012	< 0.0001	-0.036	0.016	0.03	0.0017	0.0002	< 0.0001	0.00036	0.00025	0.1661
IS	8.63	0.91	< 0.0001	-2.25	1.26	0.08	0.12	0.017	< 0.0001	0.016	0.021	0.47
Tb.Th	95.58	6.26	< 0.0001	-19.48	9.81	0.05	0.97	0.1	< 0.0001	0.37	0.1	0.0005

Mean value and standard error (SE) of β_0, β_1, β_2, β_{12} for BV, BMD, IS, and Tb.Th as well as the *p*-value from the ANCOVA test for coefficients of each parameter are given. The *p*-values lower than 0.05 are marked with light gray background. BV, BMD, IS, and Tb.Th represent bone volume, bone mineral density, interception surface, and trabecular thickness respectively. β_0 is a constant, β_1 represents the time-independent effect of loading, β_2 the loading-independent effect of time, and β_{12} the time-dependent effect of loading.
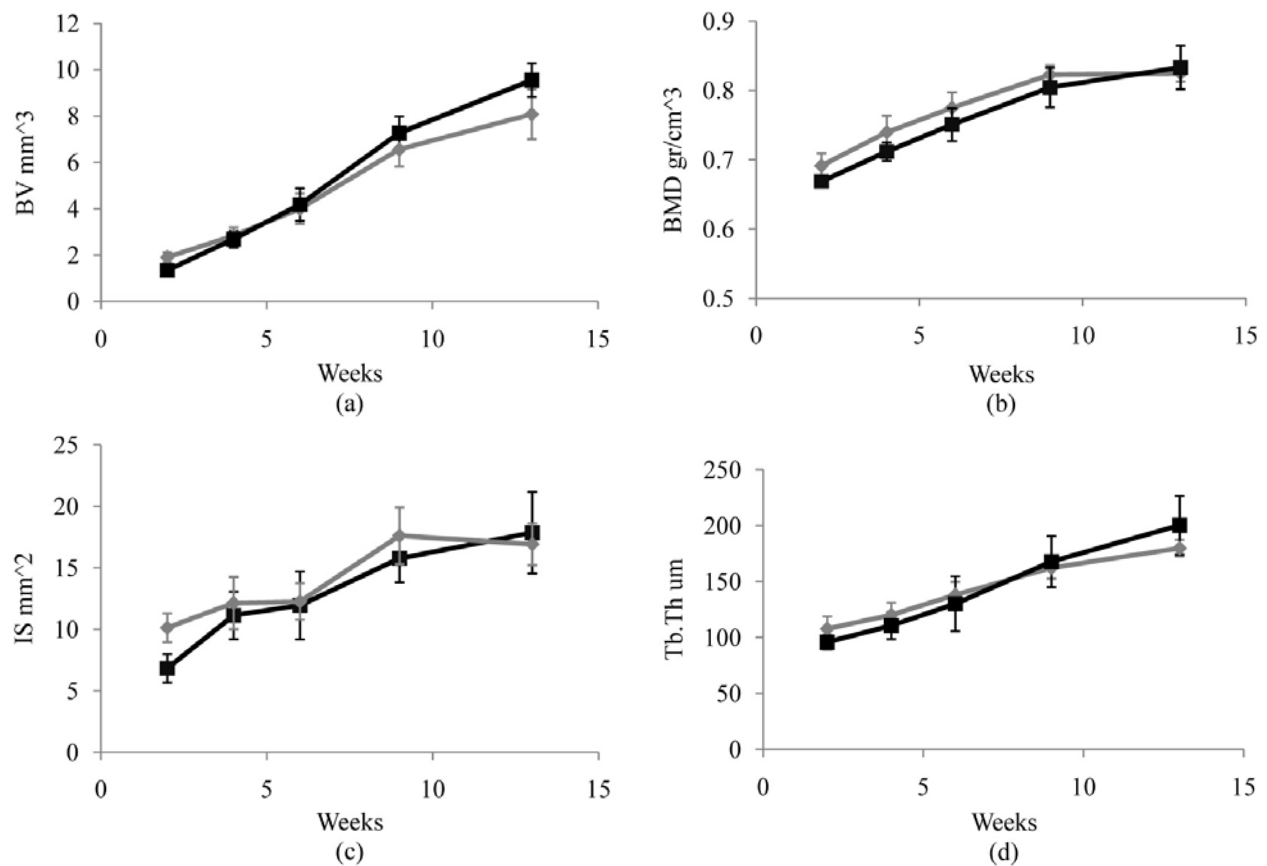
Fig. 5. The evolution of (a) BV, (b) BMD, (c) IS, and (d) Tb.Th over time for control (light gray -◆-) and loaded (black -■-) groups. All data are presented as mean ± 95% confidence interval.

Fig. 4 shows a CT slice of a loaded distal femoral epiphysis at 2 weeks and 13 weeks after the surgery. Already at 2 weeks, small amount of bone can be seen inside the scaffold that is mainly formed at the outermost part of the scaffold. We also can see callus formation around the hole in all cases at 2 weeks, which is mineralized at 4 weeks and shrunk at later time points. At 13 weeks, the new bone invades the interior of scaffold and is well spread.

Equation (2) is the estimated linear model for bone parameters as a function of time and loading

$$Y = (\beta_0 + \beta_1 F) + (\beta_2 + \beta_{12} F) T \qquad (2)$$

where Y is the estimated bone parameter, F is the dummy variable of loading which is 0 for control and 1 for loaded groups, and T is time in days. The effect of loading in eqn 2 is twofold: β_1, which is the effect of loading on Y as an intercept, and β_{12}, which is the effect of loading on the rate of change of Y.

Table 1 summarizes the estimated β_0, β_1, β_{12}, β_2 for BV, BMD, IS, and Tb.Th. The effects of loading and time on the different bone parameters are individually presented below.

Fig. 5a shows that BV in the loaded group is initially lower compared to the control group. This is reflected in the negative sign of the intercept, β_1. On the other hand, at 13 weeks, the loaded group has a higher bone volume (BV). Therefore, the rate of bone formation is higher in the loaded

group (p-value = 0.0001). Looking at the mean values of β_{12} and β_2, we conclude that the loading has enhanced the rate of bone formation by 28% ± 7%.

Looking at Fig. 5b, we see that loading induced a shift in BMD in comparison to control group. The linear mixed-effect model showed that the loading has significantly (p-value = 0.03) reduced the BMD of newly formed bone inside scaffold by 5% ± 2%.

Loading has no significant effect on intercept and rate of change of IS. Only at the first time point, a distinct difference between loaded and control group can be seen (Fig. 5c).

Fig. 5d shows that the loaded group has lower Tb.Th compared to the control group at two weeks (p-value = 0.05). However, the rate of change of Tb.Th is higher in the loaded group (38% ± 10%), which is reflected, in a highly significant effect of β_{12}.

Discussion

The goal of this study was to investigate the effect of mechanical stimulation on bone formation inside tissue engineering scaffolds. A new *in vivo* model was developed using distal femoral epiphysis of rat where a biocomposite polymeric scaffold was implanted in and later stimulated using an external loading device. *In vivo* micro-CT was used to measure newly formed bone parameters inside scaffold at several time points. To the best of the authors'

knowledge, this is the first *in vivo* model to study the effect of mechanical stimulation on scaffold that is implanted inside bone.

As bone tissue engineering is relatively a new subject, there are only few studies done on the effect of loading on bone formation inside scaffold. Duty and coworkers (Duty *et al.,* 2007) loaded a pre-seeded polymeric scaffold in a subcutaneous bone chamber and studied the effect of cyclic loading on mineralization. The advantage of the distal femur model over the subcutaneous model of Duty (Duty *et al.,* 2007) is that the scaffold is implanted inside bone. This is critical because by implanting the scaffold inside the bone, a process of healing is initiated inside the scaffold. In this process, numerous growth factors are secreted by blood cells that cause mesenchymal stromal cells to migrate from the periosteum and bone marrow into the scaffold and differentiate into osteoblasts (Davies, 2000; Muschler *et al.,* 2004). This process is absent in a subcutaneous model.

The PLA/ 5% β-TCP biocomposite scaffold was implanted without any prior cell seeding inside the scaffold. Fig. 4a shows that even two weeks after implantation, bone formation can be seen in the scaffold. This is in accordance with the results of Vehof (Vehof *et al.,* 2002), who reported the presence of bone nine days post surgery in porous scaffolds. Moreover, already at two weeks, we observed a significant amount of compact bone around the scaffold. This is not due to the compaction of trabecular bone caused by drilling, as the results of an *ex-vivo* drilling and scanning showed almost no compaction of trabecular bone around the hole (data not shown). Therefore, this perimetric compact bone is formed during the first two weeks. Although not studied here, this perimetric bone formation may have important effects on bone formation inside the scaffold. A possible effect can be stress shielding of the scaffold when it is subjected to loading, or delaying the bone healing inside scaffold due to the blocking of vasculature growth into the scaffold.

Live micro-CT scanning enabled us to study the same animals at 5 time points and hence reduced the variability and number of animals. All animals were subjected to x-ray radiation five times, which may raise some concerns about the effect of radiation on bone and surrounding tissue. As both control and loaded legs were scanned, the possible effect of radiation would be the same for all samples and cancelled by comparing loaded and control groups together. Moreover, it has been shown that *in vivo* micro-CT radiation has no significant effect on structural parameters of rat tibias and bone marrow cells after eight weekly scans (Brouwers *et al.,* 2007). In the study of Brouwers, the radiation dose for the 35 minutes scan is reported to be 0.9 Gy compared to the 0.6 Gy in our case. Moreover, in our study we scanned the animals 5 times and the duration of rest between each scan was at least two weeks. Therefore, we can conclude that the radiation doses used in the present study had no significant effects on the obtained results.

Finite element modeling was developed to determine the magnitude of loading in the *in vivo* experiment. We targeted loads that result in physiological strains inside the scaffold, based on the fact that scaffolds, as bone substitutes, are likely to be subjected to physiological loads in clinical applications. The result of the finite element model showed that 10 N of loading resulted in strains around 620 με, which is close to the strains induced in human tibia while walking (Burr *et al.,* 1996). A pilot study revealed that loads higher than 10 N were painful for the animals. Therefore, we chose 10 N as a loading magnitude for the *in vivo* study. The resulting strain within the scaffold is 20 times lower than the strain on the scaffold in the subcutaneous model of Duty (Duty *et al.,* 2007). Due to the difference in geometry and architecture of the scaffolds, these values cannot be compared directly.

The highly significant effects of intercept and time on all parameters shows the goodness of the fit of equation 1, which was expected due to the almost linear evolution of the bone parameters in time (Fig. 5 (a)-(d)). In contrast to the presented data, one would expect that the intercept be zero for all parameters, since scaffolds were empty at time zero. This shows that the linear model is not suitable for predicting the early stage of bone formation (0-2 weeks).

As can be seen in Fig. 5a, loading had a negative effect on bone formation immediately after the loading. This is an interesting finding, which is in contrast with the common belief on early load bearing of bone after surgery (Claes *et al.,* 2009). Nevertheless, the mechanical stimulation increased the rate of bone formation, which finally resulted in a higher bone volume in the loaded group. The reason for the early negative effect is not clear, but it might be due to the high stresses that were applied to the interface of the scaffold-bone, as the interception surface is also lower in loaded group at 2 weeks. A similar result has been reported in fracture healing studies where early loading of the fracture site resulted in a lower volume of callus formation in mice with osteotomized tibias (Gardner *et al.,* 2008). Using histological methods, it was found that the amount of osteoid in loaded calluses was significantly higher than in the control group. If the same phenomenon is true for the stimulated scaffolds, it may explain the later increase in bone volume. However, if the loading magnitude had been higher, the damage would have been more extensive and that would have resulted in less bone formation at later time points. Therefore excessive loading at early stages might have had a more long-term negative effect. However, on the other hand, starting the loading later on, or using moderately lower early load may resolve this problem. Further studies should be done to examine this hypothesis.

An interesting result of the present study is that only five sessions of stimulation, each lasting 5 minutes only, resulted in a significant long-term change in the rate of bone formation. To the best of the authors' knowledge, this phenomenon has never been reported for scaffold in bone. It has been reported before in bone remodeling studies where cyclic loading enhanced the rate of bone formation (Chow *et al.,* 1993; Turner *et al.,* 1995). The mechanism by which mechanical stimulation affects the rate of bone formation was not studied here, but it can be due to the effect of loading-induced fluid flow on differentiation of mesenchymal stem cells (Meinel *et al.,* 2004; Sikavitsas *et al.,* 2005; Zhao *et al.,* 2007).

BMD of the newly formed bone shows a constant increase in time, which implies that the bone is getting mature. The linear mixed effect model shows that the BMD of the loaded group is significantly lower than that of the control group (p-value<0.05). The probable reason is that due to the higher rate of bone formation, the amount of osteoid bone is also higher in the loaded group, as was seen in fracture healing (Gardner *et al.,* 2006). Therefore, presence of more immature bone decreases the mean BMD of the newly formed bone inside the scaffold. The interception surface is a measure of the connectivity of exterior bone and scaffold. As Fig. 4a shows, at two weeks after surgery, most of the bone is formed at the perimeter of the scaffold. Since at this time point the bone volume is lower in loaded group, the interception surface is also smaller. However, no significant difference was found between linear mixed-effect models of the loaded and control group. This implies that loading does not affect the interface between bone and scaffold in the long run. Trabecular thickness is a structural parameter for the newly formed bone. It is well-known that osteoblasts lay down bone layer by layer in the process of bone healing (Davies 2000) and Tb.Th represents the mean value of the thickness of the newly formed bone inside scaffold. The higher rate of change of Tb.Th shows that the process of laying bone by osteoblasts is enhanced by mechanical stimulation.

Using distal femoral epiphysis of rat as an *in vivo* model has certain advantages and disadvantages. On the downside, due to the size of the femur, the size and shape of the implanted scaffold are limited. Moreover, the magnitude of load applied to the scaffold is also limited, because excessive loads may result in damage to the knee joint. On the other hand, the small size of the rat enabled us to scan the scaffolds *in vivo* in a longitudinal study and track the changes in bone formation more precisely by reducing the sources of variation between rats and scaffolds. Another advantage of this model is that the scaffold is implanted inside trabecular bone directly, a situation similar to clinical applications.

More research is needed to characterize the effect of mechanical stimulation on bone formation in a scaffold for clinical application. There are many parameters involved in the effect of loading, and changing them may have positive or negative effects on bone formation. The magnitude and frequency of loading, for instance, are important parameters, which certainly affect the bone formation. The duration and the pattern of loading may also have important role. Moreover, the architecture and material properties of the scaffold and cell-seeding are other important aspects that possibly have interactions with the effect of the mechanical stimulation. The distal femoral epiphysis of the rat seems to be a suitable *in vivo* model for studying these different loading parameters on the bone formation in scaffold.

Conclusions

Supporting load is an important function of bone, which inevitably will be inherited by bone scaffolds. *In vitro* studies suggest that mechanical stimulation has an important role in the fate and activities of the cells inside scaffold. We employed the distal femoral epiphysis of rat with an external loading device to investigate the mechanical effect of loading on bone formation in a polymeric scaffold. We observed that on one hand, early two-week loading inhibits bone formation initially, but on the other hand it enhanced the rate of bone formation by 28% for the next 11 weeks. At the end of 13 weeks, the volume of newly-formed bone was higher in loaded scaffolds compared to the non-loaded scaffolds. The strain sustained by the scaffold was estimated to be 620 µε, at a frequency of 4 Hz. More studies are needed to fully characterize the effect of loading, and the distal femoral epiphysis of rat seems to be a suitable model for this purpose. This study showed that mechanical stimulation can be a potent enhancing signal for *in vivo* bone formation in tissue engineering scaffolds.

References

Bancroft GN, Sikavitsas VI, van den Dolder J, Sheffield TL, Ambrose CG, Jansen JA, Mikos AG (2002) Fluid flow increases mineralized matrix deposition in 3D perfusion culture of marrow stromal osteoblasts in a dose-dependent manner. Proc Natl Acad Sci USA **99**: 12600-12605.

Blecha LD (2007) Theoretical and Experimental Multi-scale Study of an Artificial Bone Construct: from Tibial Osteotomy to Cell/Fluid Interaction. Thesis, Ecole Polytechnique Federale de Lausanne.

Brouwers JE, van Rietbergen B, Huiskes R (2007) No effects of *in vivo* micro-CT radiation on structural parameters and bone marrow cells in proximal tibia of wistar rats detected after eight weekly scans. J Orthop Res **25**: 1325-1332.

Burr DB, Milgrom C, Fyhrie D, Forwood M, Nyska M, Finestone A, Hoshaw S, Saiag E, Simkin A (1996) *In vivo* measurement of human tibial strains during vigorous activity. Bone **18**: 405-410.

Cartmell SH, Porter BD, Garcia AJ, Guldberg RE (2003) Effects of medium perfusion rate on cell-seeded three-dimensional bone constructs *in vitro*. Tissue Eng **9**: 1197-1203.

Chow JW, Jagger CJ, Chambers TJ (1993) Characterization of osteogenic response to mechanical stimulation in cancellous bone of rat caudal vertebrae. Am J Physiol **265**: E340-347.

Claes L, Blakytny R, Göckelmann M, Schoen M, Ignatius A, Willie B (2009) Early dynamization by reduced fixation stiffness does not improve fracture healing in a rat femoral osteotomy model. J Orthop Res **27**: 22-27.

Davies JE (2000) Bone Engineering. Em squared Inc., Toronto, Canada.

Diggle PJ, Heagerty P, Liang K-Y and Zeger SL (2002) Analysis of Longitudinal Data, Oxford University Press, Oxford, UK.

Duty AO, Oest ME, Guldberg RE (2007) Cyclic mechanical compression increases mineralization of cell-seeded polymer scaffolds *in vivo*. J Biomech Eng **129**: 531-539.

Forwood MR, Owan I, Takano Y, Turner CH (1996) Increased bone formation in rat tibiae after a single short period of dynamic loading *in vivo*. Am J Physiol Endocrinol Metab **33**: E419-E423.

Gardner MJ, van derMeulen MC, Demetrakopoulos D, Wright TM, Myers ER, Bostrom MP (2006) *In vivo* cyclic axial compression affects bone healing in the mouse tibia. J Orthop Res **24**: 1679-1686.

Gardner MJ, Ricciardi BF, Wright TM, Bostrom MP, vanderMeulen MC (2008) Pause insertions during cyclic *in vivo* loading affect bone healing. Clin Orthop and Relat Res **466**: 1232-1238.

Goldstein AS, Juarez TM, Helmke CD, Gustin MC, Mikos AG (2001) Effect of convection on osteoblastic cell growth and function in biodegradable polymer foam scaffolds. Biomaterials **22**: 1279-1288.

Guldberg RE, Caldwell NJ, Guo XE, Goulet RW, Hollister SJ, Goldstein SA (1997) Mechanical stimulation of tissue repair in the hydraulic bone chamber. J Bone Miner Res **12**: 1295-1302.

Hogan HA, Ruhmann SP, Sampson HW (2000) The mechanical properties of cancellous bone in the proximal tibia of ovariectomized rats. J Bone Min Res 15: 284-292.

Lamerigts NMP, Buma P, Huiskes R, Schreurs W, Gardeniers J, Slooff TJJH (2000) Incorporation of morsellized bone graft under controlled loading conditions. A new animal model in the goat. Biomaterials **21**: 741-747.

Mathieu LM, Mueller TL, Bourban PE, Pioletti DP, Muller R, Manson JAE (2006) Architecture and properties of anisotropic polymer composite scaffolds for bone tissue engineering. Biomaterials **27**: 905-916.

Meinel L, Karageorgiou V, Fajardo R, Snyder B, Shinde-Patil V, Zichner L, Kaplan D, Langer R, Vunjak-Novakovic G (2004) Bone tissue engineering using human mesenchymal stem cells: Effects of scaffold material and medium flow. Ann Biomed Eng **32**: 112-122.

Montjovent MO, Mathieu L, Hinz B, Applegate LL, Bourban PE, Zambelli PY, Manson JA, Pioletti DP (2005) Biocompatibility of bioresorbable poly(L-lactic acid) composite scaffolds obtained by supercritical gas foaming with human fetal bone cells. Tissue Eng **11**: 1640-1649.

Montjovent MO, Mathieu L, Schmoekel H, Mark S, Bourban PE, Zambelli PY, Laurent-Applegate LA, Pioletti DP (2007) Repair of critical size defects in the rat cranium using ceramic-reinforced PLA scaffolds obtained by supercritical gas foaming. J Biomed Mat Res **83**: 41-51.

Montjovent MO, Mark S, Mathieu L, Scaletta C, Scherberich A, Delabarde C, Zambelli PY, Bourban PE, Applegate LA, Pioletti DP (2008) Human fetal bone cells associated with ceramic reinforced PLA scaffolds for tissue engineering. Bone **42**: 554-564.

Murakami N, Saito N, Horiuchi H, Okada T, Nozaki K, Takaoka K (2002) Repair of segmental defects in rabbit humeri with titanium fiber mesh cylinders containing recombinant human bone morphogenetic protein-2 (rhBMP-2) and a synthetic polymer. J Biomed Mater Res **62**: 169-174.

Muschler GE, Nakamoto C, Griffith LG (2004) Engineering principles of clinical cell-based tissue engineering. J Bone Joint Surg [Am] **86A**: 1541-1558.

Peter B, Gauthier O, Laib S, Bujoli B, Guicheux J, Janvier P, van Lenthe GH, Muller R, Zambelli PY, Bouler JM, Pioletti DP (2006) Local delivery of bisphosphonate from coated orthopedic implants increases implants mechanical stability in osteoporotic rats. J Biomed Mat Res **76**: 133-143.

Pinheiro JC, Bates DM (2004) Mixed-effect models in S and S-PLUS. Springer, Berlin, Germany.

Pioletti DP, Montjovent MO, Zambelli PY, Applegate L (2006) Bone tissue engineering using foetal cell therapy. Swiss Med Wkly **136**: 557-560.

Rath B, Nam J, Knobloch TJ, Lannutti JJ, Agarwal S (2008) Compressive forces induce osteogenic gene expression in calvarial osteoblasts. J Biomech **41**: 1095-1103.

Richardson TP, Peters MC, Ennett AB, Mooney DJ (2001) Polymeric system for dual growth factor delivery. Nat Biotechnol **19**: 1029-1034.

Sikavitsas VI, Bancroft GN, Holtorf HL, Jansen JA, Mikos AG (2003) Mineralized matrix deposition by marrow stromal osteoblasts in 3D perfusion culture increases with increasing fluid shear forces. Proc Natl Acad Sci USA **100**: 14683-14688.

Sikavitsas VI, Bancroft GN, Lemoine JJ, Liebschner MA, Dauner M, Mikos AG (2005) Flow perfusion enhances the calcified matrix deposition of marrow stromal cells in biodegradable nonwoven fiber mesh scaffolds. Ann Biomed Eng **33**: 63-70.

Song GB, Ju Y, Shen XD, Luo Q, Shi YS, Qin J (2007) Mechanical stretch promotes proliferation of rat bone marrow mesenchymal stem cells. Colloids Surf B **58**: 71-277.

Stadelmann VA, Hocke JM, Verhelle JR, Pioletti DP (2007) Strain distribution in mice tibia under axial loading. Numerical, experimental models. Comp Meth Biomech Biomed Eng **10** (S1): 80-90.

Tagil M, Aspenberg P (1999) Cartilage induction by controlled mechanical stimulation *in vivo*. J Orthop Res **17**: 200-204.

Tanaka SM, Sun HB, Roeder RK, Burr DB, Turner CH, Yokota H (2005) Osteoblast responses one hour after load-induced fluid flow in a three-dimensional porous matrix. Calcif Tissue Int **76**: 261-271.

Turner CH, Forwood MR, Otter MW (1994) Mechanotransduction in Bone - Do Bone-Cells Act as Sensors of Fluid-Flow. FASEB J **8**: 875-878.

Turner CH, Owan I, Takano Y (1995) Mechanotransduction in bone: role of strain rate. Am J Physiol **269**: E438-442.

van der Donk S, Buma P, Verdonschot N, Schreurs BW (2002) Effect of load on the early incorporation of impacted morsellizedallografts. Biomaterials **23**: 297-303.

van Eijk F, Saris DB, Creemers LB, Riesle J, Willems WJ, van Blitterswijk CA, Verbout AJ, Dhert WJ (2008) The effect of timing of mechanical stimulation on proliferation and differentiation of goat bone marrow stem cells cultured on braided PLGA scaffolds. Tissue Eng Part A **14**: 1425-1433.

Vehof JW, Takita H, Kuboki Y, Spauwen PH, Jansen JA (2002) Histological characterization of the early stages of bone morphogenetic protein-induced osteogenesis. J Biomed Mater Res **61**: 440-449.

Zhao F, Chella R, Ma T (2007) Effects of shear stress on 3-D human mesenchymal stem cell construct development in a perfusion bioreactor system: Experiments and hydrodynamic modeling. Biotech Bioeng **96**: 584-595.